数理解析研究所講究録
第 833 巻 1993 年 110-119

Generalized Geometric Fitting Problems and Weighted Dynamic Voronoi Diagrams

中央大学理工学部情報工学科 今井桂子 (Keiko Imai)
東京大学理学部情報科学科 今井 浩 (Hiroshi Imai)

1. Introduction

Geometric fitting two similar sets of n points is fundamental problem in image processing and pattern recognition. This minimax geometric fitting problem between two similar sets of points is considered in [10]. For example, it arises in an industrial robot attaching a pin-grid-array type LSI to a board by using visual sensors. The robot first takes an image of the pins of LSI by its visual sensor. Then it tries to fit the LSI package to the corresponding patterns on the board by geometric operations such as translation and rotation. The patterns are a collection of disks or squares of the same size. Using the furthest Voronoi diagram for moving points in the plane, this geometric fitting problem has been solved in $O(n^2\lambda_7(n)\log n)$ time [10].

In a more general setting, the following variants of the fitting problem should be considered. (a) In the case that there are some points which cannot be put into the corresponding disks, minimize the number of such points. (b) In the case that the radii of disk patterns are different from one another, solve this non-uniform geometric fitting problem (Figure 1). Recently, the Voronoi diagrams for moving objects have been investigated in connection with motion planning in robotics and geometric optimization problems[2,5,8,9,10]. In this paper, to solve the generalized problem (b), we extend the concept of the weighted Voronoi diagram for n points in the plane to the one for the case that the coordinates and the weights of each point are represented by polynomials or rational functions of a parameter. We show that the combinatorial complexity of this dynamic Voronoi diagram is $O(n^2\lambda_s(n))$ where s is some fixed number determined by the degree of the functions and $\lambda_s(n)$ is the maximum length of (n,s) Davenport-Schinzel sequence. Since a lower bound of this dynamic Voronoi diagram can be shown to be $\Omega(n^3)$, our bounds are tight within $\log^* n$ factor, which beats bounds within n^ϵ factor.

2. Generalized Geometric Fitting Problems

We here formulate the geometric fitting problems for two corresponding sets of points. The non-weighted problem has been formulated as follows [10]. Given two sets $S=\{s_j=(x_j,y_j)\mid j=1,\cdots,n\}$ and $T=\{t_j=(u_j,v_j)\mid j=1,\cdots,n\}$ of points in the plane such that s_j is associated with t_j, translate, rotate (or transform in a more complicated way) and/or scale the set S simultaneously so that the maximum of the L_2 (or L_∞) distances, according to each pattern, between t_j and the transformed s_j is minimized.

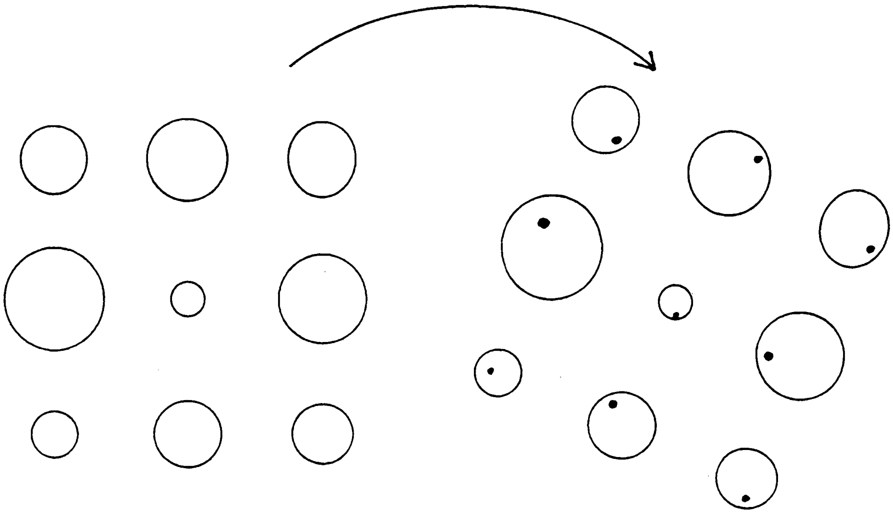

Figure 1. Geometric fitting of distorted grid points with disks with different radii

For example, in the case that the patterns are disks, and translation and rotation are used as geometric operations, the problem is expressed as follows:

$$\min_{z,0\leq\theta<2\pi} \max_{j=1,\cdots,n} \|s_j e^{i\theta} - t_j - z\| ,$$

where s_j and t_j are identified with complex numbers $x_i + iy_i$ and $u_i + iv_i$, respectively, and θ is an angle $(0 \leq \theta < 2\pi)$ and the S is translated by making the origin to $z = x + iy$. $\|\cdot\|$ denotes the Euclidean norm. Using the furthest Voronoi diagram for moving points in the plane, this geometric fitting problem can be solved in $O(n^2\lambda_7(n)\log n)$ time in L_2 norm. Defining a points $p_j(\theta)$ by $s_j e^{i\theta} - t_j$ in the complex plane, the problem is rewritten as

$$\min_{0\leq\theta<2\pi} \left(\min_{z} \max_{j=1,\cdots,n} \|p_j(\theta) - z\| \right) .$$

Fixing θ , the problem becomes the minimum enclosing circle problem for n points $p_j(\theta)$. The minimum enclosing circle problem can be solved by using the furthest Voronoi diagram.

We consider the generalized case where the radii of disk patterns are different from one another and solve this non-uniform geometric fitting problem (Figure 1). The weighted Voronoi diagram for moving points can be used to solve this generalized problem.

There are various kinds of Voronoi diagram and efficient algorithms to construct such a diagram. The weighted Voronoi diagram is one of these generalizations of the Voronoi diagram.

Let S denote a set of n weighted points p_i $(i = 1,\cdots,n)$ in the Euclidean plane. Each point p_i is associated with a non-negative real weight w_i . The weighted distance $d_i(p)$ between p_i and an arbitrary point p in $\mathbf{E}^2$ is defined by $d_i(p) = w_i\sqrt{(x-x_i)^2 + (y-y_i)^2}$, where the coordinates of p_i , p are (x_i, y_i) , (x, y) , respectively. The weighted Voronoi region of p_i is given by

$$V(p_i) = \bigcap_{i\neq j} \{p \mid d_i(p) < d_j(p)\},$$

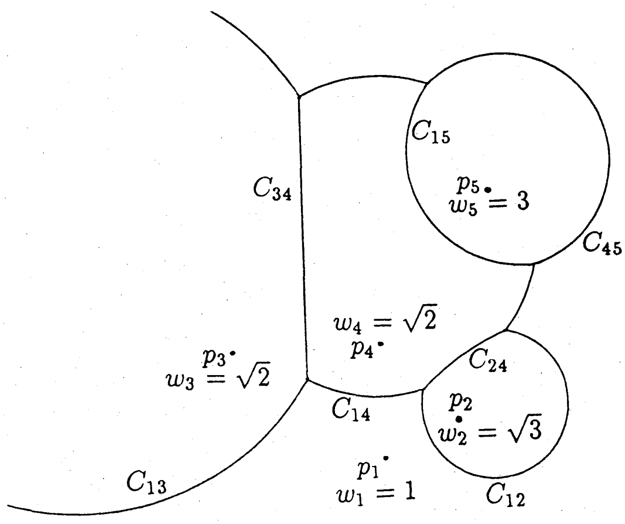

Figure 2. Weighted Voronoi diagram

and the subdivision of the Euclidean plane defined by the weighted Voronoi regions is called the weighted Voronoi diagram of S (Figure 2). The weighted Voronoi diagram for fixed n points in the plane can be constructed in $O(n^2)$ time [4]. The algorithm in [4] is optimal as the diagram can consist of $\Theta(n^2)$ faces, edges and vertices.

The weighted Voronoi diagram for moving points can be used to solve the problem (b), since the radii of the disks may be considered as weights of their centers. Suppose that point s_j should be put into disk with center t_j and radius r_j in the pattern. By rotating the set S of points by θ and further translating it by z, s_j is the corresponding disk iff $\|s_j e^{i\theta} - t_j - z\| \leq r_j$. Then, all the points in S can be put into the corresponding disks iff the following value

$$\min_{z, 0 \leq \theta < 2\pi} \max_{j=1,\cdots,n} \frac{1}{r_j} \|s_j e^{i\theta} - t_j - z\|$$

is less than or equal to 1. $\frac{1}{r_j}$ can be considered as the weight of $p_j(\theta) = s_j e^{i\theta} - t_j$. Hence, the weighted Voronoi diagram for moving points can be applied to its generalized geometric fitting problems.

To solve the geometric fitting problems, we need the weighted furthest Voronoi diagram. Although the furthest Voronoi diagram is different from the nearest one, the below arguments hold with a slight modification. Hence, we consider the dynamic nearest Voronoi diagram in the below arguments.

3. Definitions and Some Properties of the Weighted Dynamic Voronoi Diagram

In the weighted Voronoi Diagram, if the regions of two point p_i and p_j intersect each other, then the intersection is a subset of the curve defined by the equation $d_i(p) = d_j(p)$. The equidistant curve from p_i and p_j is a circle, and one of the points p_i, p_j whose weight is greater than that of the other is enclosed in the circle, which is called the

Apollonius' circle for p_i and p_j . Let p_{ij} be the center of the circle C_{ij} and r_{ij} be its radius:

$$p_{ij} = \left(\frac{w_i^2 x_i - w_j^2 x_j}{w_i^2 - w_j^2}, \frac{w_i^2 y_i - w_j^2 y_j}{w_i^2 - w_j^2} \right), \quad r_{ij} = \frac{w_i w_j}{|w_i^2 - w_j^2|} \sqrt{(x_i - x_j)^2 + (y_i - y_j)^2}.$$

Note here that the equidistant curve from the two points with same weights is a line.

In the weighted Voronoi diagram, the set of the equidistants from three points of S consists of at most two points. See Figure 2.

For each i ,

$$z = f_i(x, y) = w_i \sqrt{(x - x_i)^2 + (y - y_i)^2}$$

is a cone with the singular point at $(x_i, y_i, 0)$. When the cone $z = f_i(x, y)$ intersects another cone $z = f_j(x, y)$, the intersection of two cones is a quadratic curve in $\mathbf{E}^3$. The projection of the quadratic curve is nothing but the Apollonius' circle for p_i , p_j . Consider the lower envelope of the graphs of n functions $f_i(x, y)$. Projecting down this lower envelope to the (x, y) -plane yields the weighted Voronoi diagram for n points p_i .

The weighted Voronoi diagram may be extended to that for moving points in the following way. Consider n points $p_i(t) = (x_i(t), y_i(t))$ with weights $w_i(t)$ parametrized by t in the plane, where $x_i(t)$, $y_i(t)$ and $w_i(t)$ are functions of t , which are polynomials or rational functions of t . The degrees of these functions are assumed to be independent of n . To simplify our discussion, it is also assumed that these functions are different from one another. As we mentioned before, for fixed t , the weighted Voronoi diagram for $p_i(t)$ is the orthogonal projection of the lower envelope of functions $z = f_i(x, y) = w_i \sqrt{(x - x_i)^2 + (y - y_i)^2}$ of two variables x and y . In a similar way, the problem of constructing the weighted dynamic diagram may be regarded as computing the lower envelope of n functions

$$f_i(x, y, t) = w_i(t) \sqrt{(x - x_i(t))^2 + (y - y_i(t))^2}$$

of three variables x , y and t . Define $f(x, y, t)$ by

$$f(x, y, t) = \min_{i=1,\cdots,n} f_i(x, y, t).$$

Now the problem is how to compute $f(x, y, t)$.

For this function $f(x, y, t)$, the *minimum diagram* is a subdivision of (x, y, t) -space such that, with each region, a function f_i attaining the minimum in the definition of f for any point in the region is associated. This is nothing but the projection of the pointwise minimum of these functions onto the (x, y, t) -space. The intersection of this diagram with the plane $t = t_0$ is a weighted Voronoi diagram for $t = t_0$, and the whole diagram is called the *weighted dynamic Voronoi diagram.*

By the assumptions on $p_i(t)$, each region of the minimum diagram of f consists of a maximal connected 3-dimensional set of points at which the minimum is attained by a function f_i . The faces, edges and vertices of the subdivision consist of points at which the minimum is attained simultaneously by two, three and four, respectively, functions. It is easy to see the following properties of the intersections of the trivariate functions $f_i(x,y,t)$ by solving the simultaneous equations each of which defines a function $f_i(x,y,t)$ in the 4-dimensional Euclidean space $\mathbf{E}^4$. In the sequel, variables x , y , t of f_i will be often omitted.

Lemma 1: (1) For each $i \neq j$, $f_i(t,x,y) = f_j(t,x,y)$ is a connected surface in $\mathbf{E}^4$.
(2) For each triple i , j , k of distinct indices, $f_i(t) = f_j(t) = f_k(t)$ consists of at most two points for fixed t and $f_i = f_j = f_k$ is a curve with parameter t . The curve has at most two components and is discontinuous at most constant times.
(3) For four distinct indices i , j , k and l , $f_i = f_j = f_k = f_l$ consists of at most s points, where s is a constant. □

4. Combinatorial Complexity of the Minimum Diagram and Constructing the Diagram

A trivial bound on the number of vertices on the minimum diagram is $O(n^4)$, since the number of vertices is bounded by $s\binom{n}{4}$ by Lemma 1. However, this is loose as shown below.

Let i and j be distinct two indices, and fix them. Let l_{ij} be the oriented line passing $p_i(t)$ and $p_j(t)$ and the orientation is defined as follows. When weight of p_i is less than that of p_j , l_{ij} is oriented from p_i to p_j . There are two points on the oriented line which are at equal distances from $p_i(t)$ and $p_j(t)$. One of the two points is between $p_i(t)$ and $p_j(t)$ and the point is denoted by m_{ij} . The other is denoted by $\widetilde{m}_{ij}$. See Figure 3(a). Draw the circle C_{jk} for each $k \neq i,j$ and consider the intersection points of C_{ij} , C_{jk} . Those intersection points are nothing but the equidistants from p_i , p_j , p_k . Using the intersection points of C_{ij} , C_{jk} , we define four points $q_k^+(t)$, $q_k^-(t)$, $\tilde{q}_k^+(t)$ and $\tilde{q}_k^-(t)$ as follows. $d_E(p,q)$ is the Euclidean distance between p and q .

Case 1: $d_E(p_{ij},p_{jk}) < r_{ij} + r_{jk}$ and $d_E(p_{ij},p_{jk}) > |r_{ij} - r_{jk}|$.

In this case, C_{ij} intersects C_{jk} at two points q and q' . Let s_k be the line segment connecting q and q' .

Case 1-1: $s_k \cap l_{ij} = \emptyset$.

Case 1-1-1: Consider the case where C_{jk} intersects l_{ij} and these two intersection points are between m_{ij} and $\widetilde{m}_{ij}$. When the segment is on the right side of l_{ij} , choose the point which is counterclockwisely nearer along the circle from m_{ij} between q and q' and let q_k^- be the point and q_k^+ be the other. See Figure 3(a). When the

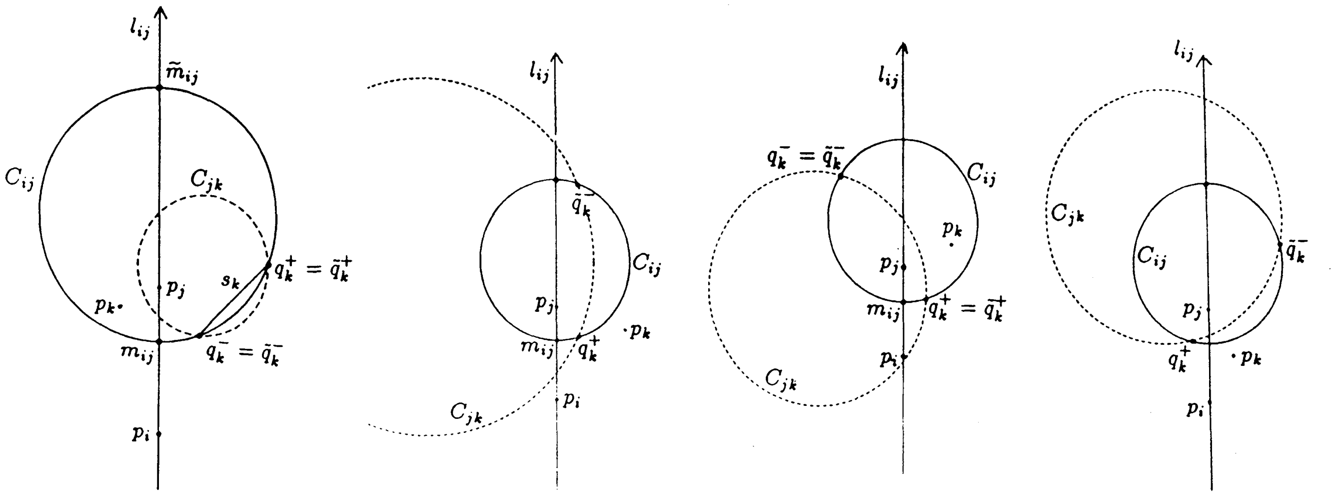

(a) Case 1-1-1 (b) Case 1-1-2 (c) Case 1-2-1 (d) Case 1-2-2

Figure 3. Definitions of q_k^+ , q_k^- , $\tilde{q}_k^+$ and $\tilde{q}_k^-$

segment is on the left side of l_{ij} , choose the point which is clockwisely nearer along the circle from m_{ij} and let q_k^+ be the point and q_k^- be the other. Moreover, we define $\tilde{q}_k^+ = q_k^+$, $\tilde{q}_k^- = q_k^-$.

Case 1-1-2: Consider the case where C_{jk} does not intersect l_{ij} , or C_{jk} intersects l_{ij} at two points and m_{ij} , $\widetilde{m}_{ij}$ are between those two points. When the segment is on the right side of l_{ij} , choose the point which is counterclockwisely nearer along the circle from m_{ij} between q and q' and let q_k^+ be the point and $\tilde{q}_k^-$ be the other. Furthermore, we define $\tilde{q}_k^+ = +\infty$, $q_k^- = -\infty$. If $\tilde{q}_k^- = \widetilde{m}_{ij}$, then we consider $\tilde{q}_k^- = +\widetilde{m}_{ij}$, where $\pm\widetilde{m}_{ij}$ are the point $\widetilde{m}_{ij}$ and we assume $+\widetilde{m}_{ij}$ (resp. $-\widetilde{m}_{ij}$) is on the right (resp. left) side of l_{ij} . See Figure 3(b). When the segment is on the left side of l_{ij} , choose the point which is clockwisely nearer along the circle from m_{ij} between q and q' and let q_k^- be the point and $\tilde{q}_k^+$ be the other. Furthermore, we define $q_k^+ = +\infty$, $\tilde{q}_k^- = -\infty$. If $\tilde{q}_k^+ = \widetilde{m}_{ij}$, then we consider $\tilde{q}_k^+ = -\widetilde{m}_{ij}$.

Case 1-2: $s_k \cap l_{ij} \neq \emptyset$.

l_{ij} intersects C_{ik} at two points.

Case 1-2-1: Consider the case where $w_j > w_k$ and m_{ij} is between these intersection points of l_{ij} and C_{jk} , or $w_j < w_k$ and $\widetilde{m}_{ij}$ is between these intersection points of l_{ij} and C_{jk} . Define the point lying on the right side of l_{ij} among q and q' to be q_k^+ . The other point, lying on the left side of l_{ij} , is called q_k^- . We define $\tilde{q}_k^+$ and $\tilde{q}_k^-$ as $\tilde{q}_k^+ = q_k^+$, $\tilde{q}_k^- = q_k^-$. See Figure 3(c).

Case 1-2-2: Consider the case where $w_j > w_k$ and $\widetilde{m}_{ij}$ is between these intersection points of l_{ij} and C_{jk} , or $w_j < w_k$ and m_{ij} is between these intersection points of l_{ij} and C_{jk}. Define the point lying on the right side of l_{ij} among q and q' to be $\tilde{q}_k^-$. The other point, lying on the left side of l_{ij}, is called q_k^+. Set $\tilde{q}_k^+ = +\infty$, $q_k^- = -\infty$. See Figure 3(d). If $\tilde{q}_k^- = \widetilde{m}_{ij}$ (resp. $q_k^+ = \widetilde{m}_{ij}$), then we consider $\tilde{q}_k^- = +\widetilde{m}_{ij}$ (resp. $q_k^+ = -\widetilde{m}_{ij}$).

Case 2: $d_E(p_{ij}, p_{jk}) = r_{ij} + r_{jk}$.

In this case, there is only one intersection point of C_{ij} and C_{jk}. We call the intersection point q and define four points by $q_k^+ = q_k^- = \tilde{q}_k^+ = \tilde{q}_k^- = q$.

Case 3: $d_E(p_{ij}, p_{jk}) > r_{ij} + r_{jk}$ or $d_E(p_{ij}, p_{jk}) < |r_{ij} - r_{jk}|$.

There is no intersection point of C_{ij} and C_{ik}.

Case 3-1: In the cases that $d_E(p_{ij} - p_{jk}) > r_{ij} + r_{jk}$ or $d_E(p_{ij} - p_{jk}) < -r_{ij} + r_{jk}$, the four points are defined by $q_k^+ = \tilde{q}_k^+ = +\infty$, $q_k^- = \tilde{q}_k^- = -\infty$.

Case 3-2: If $d_E(p_{ij} - p_{jk}) < r_{ij} - r_{jk}$, we set $q_k^+ = \tilde{q}_k^+ = -\infty$, $q_k^- = \tilde{q}_k^- = +\infty$.

Let d_k^- (d_k^+, $\tilde{d}_k^-$, $\tilde{d}_k^+$) be the Euclid distance between p_{ij} and q_k^- (q_k^+, $\tilde{q}_k^-$, $\tilde{q}_k^+$). We consider the distance between a point and $\pm\infty$ is infinity and the point $+\infty$ (resp. $-\infty$) is on the right (resp. left) side of $l_{ij}(t)$. We define four functions g_k^+, g_k^-, $\tilde{g}_k^+$ and $\tilde{g}_k^-$ by using four points q_k^+, q_k^-, $\tilde{q}_k^+$ and $\tilde{q}_k^-$ as follows.

$$g_k^+(t) = \begin{cases} +d_k^+ & (q_k^+ \text{ is on the right side of } l_{ij}(t)) \\ -d_k^+ & (q_k^+ \text{ is on the left side of } l_{ij}(t)) \end{cases}$$

$$g_k^-(t) = \begin{cases} -d_k^- & (q_k^- \text{ is on the right side of } l_{ij}(t)) \\ +d_k^- & (q_k^- \text{ is on the left side of } l_{ij}(t)) \end{cases}$$

$$\tilde{g}_k^+(t) = \begin{cases} +\tilde{d}_k^+ & (\tilde{q}_k^+ \text{ is on the right side of } l_{ij}(t)) \\ -\tilde{d}_k^+ & (\tilde{q}_k^+ \text{ is on the left side of } l_{ij}(t)) \end{cases}$$

$$\tilde{g}_k^-(t) = \begin{cases} -\tilde{d}_k^- & (\tilde{q}_k^- \text{ is on the right side of } l_{ij}(t)) \\ +\tilde{d}_k^- & (\tilde{q}_k^- \text{ is on the left side of } l_{ij}(t)) \end{cases}$$

For $g_k^+(t)$, $g_k^-(t)$, $\tilde{g}_k^+(t)$, $\tilde{g}_k^-(t)$, further define $g^+(t)$, $g^-(t)$, $g'(t)$, $\tilde{g}^+(t)$, $\tilde{g}^-(t)$ and $\tilde{g}'(t)$ as follows:

$$g^+(t) = \min_{k \neq i,j} g_k^+(t), \qquad \tilde{g}^+(t) = \min_{k \neq i,j} \tilde{g}_k^+(t),$$

$$g^-(t) = \min_{k \neq i,j} g_k^-(t), \qquad \tilde{g}^-(t) = \min_{k \neq i,j} \tilde{g}_k^-(t),$$

$$g'(t) = \max\{g^-(t) + g^+(t), 0\}, \quad \tilde{g}'(t) = \max\{\tilde{g}^-(t) + \tilde{g}^+(t), 0\}.$$

$$h(t) = \max\{g^+(t) - \tilde{g}^-(t), 0\}$$

Geometric implications of these definitions are given by the following lemma. Note that Voronoi edge E_{ij}, which is on the boundary of Voronoi regions V_i, V_j, may be disconnected and may consist of some connected components $\{e_{ij}\}$.

Lemma 2: (1) For t, suppose $g'(t) > 0$, $g^+(t) \neq \pm\infty$ (resp. $g^-(t) \neq \pm\infty$) is attained by a function $g_k^+(t)$ (resp. $g_l^-(t)$). Then, $q_k^+(t)$ and $q_l^-(t)$ are Voronoi points which are

on the boundaries of Voronoi regions V_i , V_j , V_k (V_l) , and equidistant from p_i , p_j , p_k (p_l) . $q_k^+(t)$ (resp. $q_l^-(t)$) is the right (resp. left) end point of the leftest component e_{ij} of E_{ij} regarding the orientation defined the oriented line l_{ij} and the point m_{ij} .
(2) For t , suppose $\tilde{g}'(t) > 0$, $\tilde{g}^+(t) \neq \pm\infty$ (resp. $\tilde{g}^-(t) \neq \pm\infty$) is attained by a function $\tilde{g}_k^+(t)$ (resp. $\tilde{g}_l^-(t)$). Then, $q_k^+(t)$ and $q_l^-(t)$ are Voronoi points which are on the boundaries of Voronoi regions V_i , V_j , V_k (V_l) , and equidistant from p_i , p_j , p_k (p_l) . $q_k^+(t)$ (resp. $q_l^-(t)$) is the right (resp. left) end point of the rightest component e_{ij} of E_{ij} regarding the orientation defined the oriented line l_{ij} and the point m_{ij} . □

Graphs of g^+ , g^- and g' are composed of maximal connected portions of graphs of g_k^+ , g_k^- , $g_k^+ + g_l^-$ and 0 . As usual, define the combinatorial complexity of these functions to be the maximum number of such maximal connected portions. Also, call t' an intersecting value of a function (g^+ , g^- , g') if the functions (g_k^+ , g_k^- , $g_k^+ + g_l^-$, 0) attaining its minimum at $t' - t_\epsilon$ and $t' + t_\epsilon$ are different for sufficiently small t_ϵ . The number of intersecting values is nearly equal to the combinatorial complexity. This complexity can be evaluated as follows, where $\lambda_s(n)$ is the maximum length of (n, s) Davenport-Schinzel sequence (e.g., see [1,3,6,11,12]), and is almost linear in n . For $\tilde{q}^+$, $\tilde{q}^-$, $\tilde{q}'$ and h , similar.

Lemma 3: The combinatorial complexity of g^+ , g^- and g' ($\tilde{g}^+$, $\tilde{g}^-$ and $\tilde{g}'$) are $O(\lambda_{s+2}(n))$. These functions can be computed in $O(\lambda_{s+1}(n) \log n)$ time and $O(n)$ space.
Proof: Each g_k^+ may be discontinuous at most a constant number of times from Lemma 1(2). Any two functions among g_k^+ intersect at most s points from Lemma 1(3). Hence, the combinatorial complexity of g^+ is $O(\lambda_{s+2}(n))$ [3]. For g^- , similar. Any two functions among g_k^+ , g_k^- , $g_k^+ + g_l^-$ and 0 intersect at most constant times. Then, the combinatorial complexity of g' is within that of g^+ and g^- by a constant factor. The time complexity follows from [7]. For $\tilde{g}^+$, $\tilde{g}^-$ and $\tilde{g}'$, similar. For h , the graph of h are composed of maximal connected portions of graphs of g_k^+ , $\tilde{g}_l^-$, $g_k^+ - \tilde{g}_l^-$ and 0 . Any two functions among these functions also intersect at most constant times. Hence, the combinatorial complexity of h is within that of g^+ and $\tilde{g}^-$ by a constant factor. □

Fixing i and j , the end points of the leftest and rightest components of Voronoi edge E_{ij} regarding the orientation defined by the oriented line l_{ij} and the middle point m_{ij} , are the points q , q' associated with the function g^+ , g^- , $\tilde{g}^+$, $\tilde{g}^-$. However, some of the Voronoi points on E_{ij} may be incident to the components of E_{ij} which are not the leftest or rightest ones. Such Voronoi points cannot be listed by using the functions g^+ , g^- , $\tilde{g}^+$ and $\tilde{g}^-$ for the indices i , j . The remaining problem is how to maintain such Voronoi points and count the topological changes. We assume that q is the Voronoi point which is the end points of neither of the leftest and rightest components and $w_i < w_j < w_k$. In this case, we choose the indices j and k instead of i and j, and define the functions g^+, g^-, $\tilde{g}^+$, $\tilde{g}^-$ for new indices j and k. It is easily to see that the point is the end points of the leftest and rightest components of Voronoi edge E_{jk} regarding the orientation defined by the oriented line l_{jk} and the middle point m_{jk}. Therefore, any end point of Voronoi edge is the end point of the leftest and rightest component regarding the orientation defined by the oriented line $l_{i'j'}$ and the middle point $m_{i'j'}$ for a pair of indices i', j'.

Theorem 1: The weighted dynamic Voronoi diagram has the combinatorial complexity of $O(n^2\lambda_{s+2}(n))$, and can be computed in $O(n^2\lambda_{s+1}(n)\log n)$ time and $O(n)$ space.
Proof: Suppose that one of the intersections, whose number is at most s, of f_i, f_j, f_k and f_l in $\mathbf{E}^4$ correspondis to a vertex on the minimum diagram in $\mathbf{E}^3$, and the t-coordinate of this point is t'. There exists a point q which is equidistant from $p_i(t')$, $p_j(t')$, $p_k(t')$, $p_l(t')$, and, for the other indices h, $p_h(t')$ is farther from q than these four points. For $t'-t_\epsilon$ (for sufficiently small t_ϵ), $q(t'-t_\epsilon)$ is the end points of the leftest or rightest component of one of the sets E_{ij}, E_{ik}, E_{il}, E_{jk}, E_{jl} and E_{kl}. Suppose $q(t'-t_\epsilon)$ is the end point of the leftest or rightest edge in E_{ij}, then t' is an intersecting value of one of the functions g^+, g^-, g', $\tilde{g}^+$, $\tilde{g}^-$, $\tilde{g}'$ and h defined for the indices i and j. Therefore, any vertex on the minimum diagram is associated with a intersecting value of one of the functions g^+, g^-, $\tilde{g}^+$ and $\tilde{g}^-$, or with a solution of one of the equations $g^+ + g^- = 0$, $\tilde{g}^+ + \tilde{g}^- = 0$ and $g^+ - \tilde{g}^- = 0$. When $q = \widetilde{m}_{ij}$, then it is associated with a solution of $g^+ - \tilde{g}^- = 0$. Conversely, each of such intersecting values corresponds to a unique vertex in the minimum diagram. A solution of $g^+ - \tilde{g}^- = 0$ corresponds to a vertex in the minimum diagram in the case that $g^- = +\infty$, $\tilde{g}^+ = +\infty$ and $g^+ = \tilde{g}^- = 2r_{ij}$.

Hence, the combinatorial complexity of the weighted dynamic Voronoi diagram is $O(n^2\lambda_{s+2}(n))$. By computing g^+, g^-, g', $\tilde{g}^+$, $\tilde{g}^-$, $\tilde{g}'$, h for any pair of $p_i(t)$ and $p_j(t)$, all the vertices on the weighted Voronoi diagram can be listed in $O(n^2\lambda_{s+1}(n)\log n)$ time and $O(n)$ space. □

5. Conclusion

In this paper, we extend the concept of the weighted Voronoi diagram for n points to the one for the case that the coordinates of each point and the weights are represented by polynomials or rational functions of a parameter. We show that combinatorial complexity of this dynamic Voronoi diagram is $O(n^2\lambda_s(n))$ where s is some fixed number determined by the degree of the functions and $\lambda_s(n)$ is the maximum length of (n, s) Davenport-Schinzel sequence. Since a lower bound of this dynamic Voronoi diagram can be shown to be $\Omega(n^3)$, our bounds are tight within $\log^* n$ factor, which beats bounds within n^ϵ factor.

Applications of these dynamic Voronoi diagrams to some generlized geometric fitting problems are also presented. As related problems, constructing the higher-order Voronoi diagram for moving points in the plane and the dynamic Voronoi diagram for n circles in the Euclidean geometry and in the Laguerre geometry can be considered. For these problems, using the same technique presented in this paper, we obtain an $O(n^2\lambda_{s+1}(n)\log n)$ algorithm for moving circles in Euclidean and Laguerre geometry, and an $O(n^2 m\lambda_{s+m+2}(n)\log n)$ algorithm for the dynamic m-th Voronoi diagram.

References

[1] P. K. Agarwal, M. Sharir and P. Shor: Sharp Upper and Lower Bounds for the Length of General Davenport-Schinzel Sequences. *Journal of Combinatorial Theory, Series A*, Vol. 52 (1989), pp.228–274.

[2] H. Aonuma, H. Imai, K. Imai and T. Tokuyama: Maximin Location of Convex Objects in a Polygon and Related Dynamic Voronoi Diagrams. *Proceedings of the 6th Annual ACM Symposium on Computational Geometry*, 1990, pp.225–234.

[3] M. J. Atallah: Some Dynamic Computational Geometry Problems. *Computers and Mathematics with Applications*, Vol.11 (1985), pp.1171–1181.

[4] F. Aurenhammer and H. Edelsbrunner: An Optimal Algorithm for Constructing the Weighted Voronoi Diagram in the Plane. *Pattern Recognition*, Vol. 17 (1984), pp.251–257.

[5] L. P. Chew and K. Kedem: Placing the Largest Similar Copy of a Convex Polygon. *Proceedings of the 5th Anuual ACM Symposium on Computational Geometry*, 1989, pp.167–174.

[6] H. Edelsbrunner, J. Pach, J. T. Schwartz and M. Sharir: On the Lower Envelope of Bivariate Functions and Its Applications. *Proceedings of the 28th IEEE Annual Symposium on Foundations of Computer Science*, 1987, pp.27–37.

[7] J. Hershberger: Finding the Upper Envelope of n Line Segments in $O(n \log n)$ Time. *Information Processing Letters.*

[8] K. Imai: Voronoi Diagrams for Moving Points and its Applications (in Japanese). *Transactions of the Japan Society for Industrial and Applied Mathematics*, Vol. 1 (1991), pp.127–134.

[9] K. Imai and H. Imai: Higher-Order Dynamic Voronoi Diagrams and its Applications (in Japanese). *Memoirs of Mathematical Research Institute,*, Kyoto University, Vol. 790, 1992, pp.222–228.

[10] K. Imai, S. Sumino and H. Imai: Geometric Fitting of Two Corresponding Sets of Points. *Proceedings of the 5th Anuual ACM Symposium on Computational Geometry*, 1989, pp.266–275.

[11] J. T. Schwartz and M. Sharir: On the Two-Dimensional Davenport-Schinzel Problem. *Journal of Symbolic Computation*, Vol.10 (1990), pp.371–393.

[12] E. Szemeredi: On a Problem by Davenport and Schinzel. *Acta Arithmetica*, Vol. 25 (1974), pp.213–224.